Article published in:

Proc. SPIE 10494, Photons Plus Ultrasound: Imaging and Sensing 2018, 104941C (19 February 2018)

The publication is available at SPIE via

https://doi.org/10.1117/12.2288362

PROCEEDINGS OF SPIE

SPIEDigitalLibrary.org/conference-proceedings-of-spie

Confidence estimation for quantitative photoacoustic imaging

Janek Gröhl, Thomas Kirchner, Lena Maier-Hein

Janek Gröhl, Thomas Kirchner, Lena Maier-Hein, "Confidence estimation for quantitative photoacoustic imaging," Proc. SPIE 10494, Photons Plus Ultrasound: Imaging and Sensing 2018, 104941C (19 February 2018); doi: 10.1117/12.2288362

SPIE.

Event: SPIE BiOS, 2018, San Francisco, California, United States

Confidence estimation for quantitative photoacoustic imaging

Janek Gröhl[a,b], Thomas Kirchner[a,c], and Lena Maier-Hein[a,b]

[a]Division of Computer Assisted Medical Interventions (CAMI), German Cancer Research Center (DKFZ), Heidelberg, Germany
[b]Medical Faculty, Heidelberg University, Germany
[c]Faculty of Physics and Astronomy, Heidelberg University, Germany

ABSTRACT

Quantification of photoacoustic (PA) images is one of the major challenges currently being addressed in PA research. Tissue properties can be quantified by correcting the recorded PA signal with an estimation of the corresponding fluence. Fluence estimation itself, however, is an ill-posed inverse problem which usually needs simplifying assumptions to be solved with state-of-the-art methods. These simplifications, as well as noise and artifacts in PA images reduce the accuracy of quantitative PA imaging (PAI). This reduction in accuracy is often localized to image regions where the assumptions do not hold true. This impedes the reconstruction of functional parameters when averaging over entire regions of interest (ROI). Averaging over a subset of voxels with a high accuracy would lead to an improved estimation of such parameters. To achieve this, we propose a novel approach to the local estimation of confidence in quantitative reconstructions of PA images. It makes use of conditional probability densities to estimate confidence intervals alongside the actual quantification. It encapsulates an estimation of the errors introduced by fluence estimation as well as signal noise. We validate the approach using Monte Carlo generated data in combination with a recently introduced machine learning-based approach to quantitative PAI. Our experiments show at least a two-fold improvement in quantification accuracy when evaluating on voxels with high confidence instead of thresholding signal intensity.

Keywords: confidence, uncertainty estimation, quantitative imaging

1. INTRODUCTION

Accurate signal quantification of photoacoustic (PA) images could have a high impact on clinical PA applications[1,2,3] but despite of the recent progress in the field towards quantitative PA imaging (qPAI), it still remains a major challenge yet to be addressed.[4,5,6,7,8] Optical absorption can be quantitatively extracted from a recorded PA signal by correcting it with an estimation of the light fluence. Fluence estimation is an ill-posed inverse problem that needs simplifying assumptions to be solved with state-of-the-art methods.[9] A breakdown of these assumptions has a negative impact on the quantification result. As suggested by prior work,[10,11] a better understanding of the underlying uncertainties of these methods could improve quantification accuracy. This is especially true for machine learning methods, as the space of possible optical parameter distributions is huge and lack of representative training data is a primary source of uncertainty.

In clinical applications, physicians need to be able to trust the quantification results, as high quantification errors could lead to unfavourable decisions for the patient. In particular, when using the quantified signal to derive functional parameters such as blood oxygen saturation inaccurate quantification results might lead to misdiagnosis. One way to attenuate this risk would be to provide an estimation of confidence that reflects the uncertainty alongside the quantification results. Such a confidence metric would provide the ability to decide whether to trust a certain result or whether to take further diagnostic steps. In an ideal case, low confidence values would always correspond to high quantification errors and vice versa. The estimation of uncertainty is vastly used in applied computer sciences[12,13,14,15,16,17,18] and also recently in the field of PAI,[10,11,19] but it was not shown how to use the acquired uncertainty information to improve the accuracy of quantification methods.

Further author information: (Send correspondence to J.G. or L.M.H.)
J.G.: E-mail: j.groehl@dkfz-heidelberg.de
L.M.H.: E-mail: l.maier-hein@dkfz-heidelberg.de

Photons Plus Ultrasound: Imaging and Sensing 2018, edited by Alexander A. Oraevsky, Lihong V. Wang, Proc. of SPIE Vol. 10494, 104941C · © 2018 SPIE · CCC code: 1605-7422/18/$18 · doi: 10.1117/12.2288362

In this contribution we present a confidence metric that is able to represent quantification uncertainty in qPAI and thus makes it possible to improve accuracy by only evaluating confident quantification estimations. We quantify optical absorption in an *in silico* dataset with a machine learning-based approach presented previously[20] and show that using a confidence metric to threshold regions of interest can greatly improve quantification accuracy if the evaluation is only performed on voxels with a high confidence value.

2. METHODS

We use a machine learning-based model (cf. section 2.1) to derive quantitative information of optical absorption μ_a from the measured signal corresponding to the initial pressure distribution. Figure 1 illustrates that there are two main sources of uncertainty during the quantification process: (1) aleatoric uncertainty corresponding to noise and artifacts of the signal and (2) epistemic uncertainty referring to errors introduced by the quantification model.[12,21] As such, we propose a joint confidence metric that encompasses both epistemic as well as aleatoric uncertainty which can be used to choose a region of interest corresponding to contain highly confident quantification estimates only.

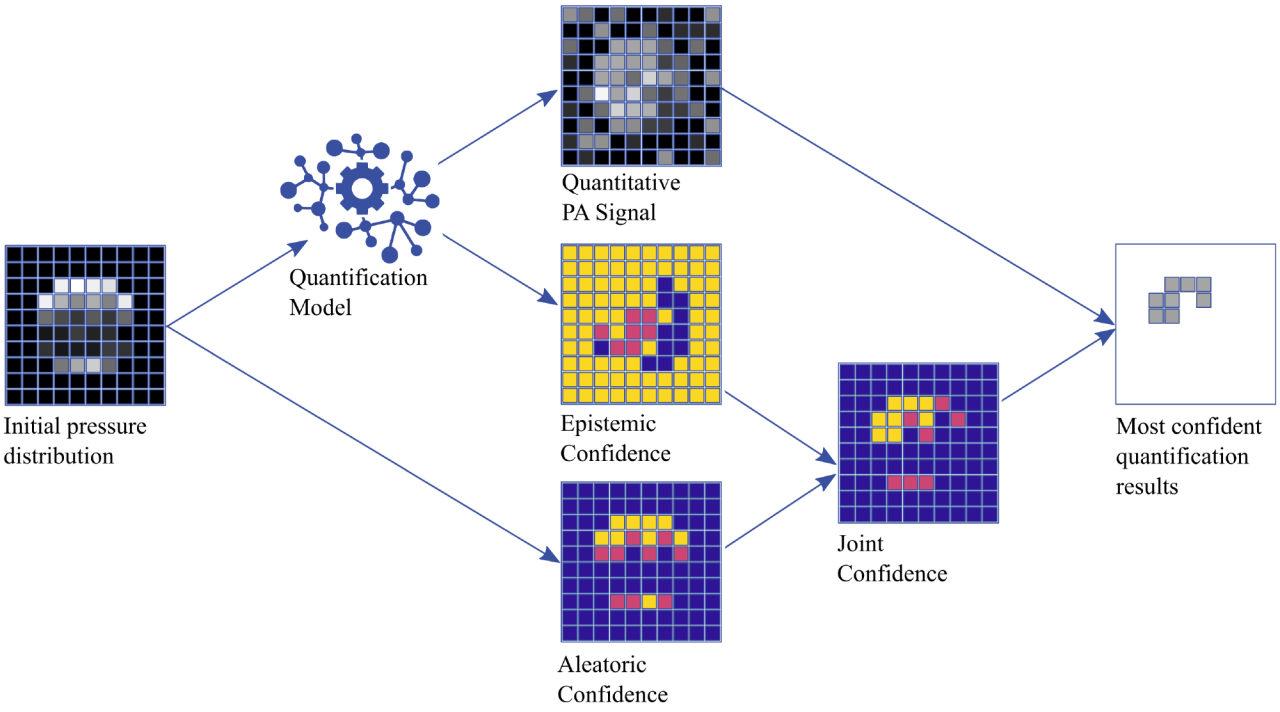

Figure 1. Overview over the proposed approach to confidence estimation of quantification results. A joint confidence metric is proposed to select only the most confident quantification results for evaluation. The joint confidence is composed of an epistemic (model based) confidence metric as well as an aleatoric confidence metric that reflects the noise of the measured signal. In this graphic, bright and yellow colors correspond to high confidence, red tones to medium confidence, and darker blue colors correspond to low confidence. The signal of the initial pressure distribution is quantified using a quantification model presented in our previous work.[20]

2.1 Signal quantification model

Using a previously presented machine learning-based method, we estimate the fluence from a 3D signal S on a voxel level and use this fluence estimate to correct the signal in the imaging plane.[20] In this method, we use feature vectors that encode both the 3D signal context of the PA image and the properties of the imaging system specifically for each voxel in the imaging plane. As labels we use a fluence correction term which is defined as $\phi_c(v) = \phi(v)/\phi_h(v)$, where $\phi_h(v)$ is a simulation based solely on a homogeneous background tissue assumption. During training, the model is given tuples of feature vectors and corresponding labels for each

voxel in the training dataset. For quantification of a voxel v of an unseen 3D image, the voxel-specific feature vector is generated from the image and used to estimate the fluence $\hat{\phi}(v)$ in that voxel with the trained model. The absorption coefficient $\hat{\mu}_a(v)$ is then estimated with $\hat{\mu}_a(v) = S(v)/(\hat{\phi}(v) \cdot \Gamma)$ where we assume a constant Grueneisen coefficient Γ.

In this contribution, we introduce an adaptation to the previously presented quantification method in order to be able to represent estimation uncertainty. Our implementation of this is based on the work of Feindt[13] and uses cumulative probability distribution functions (CDFs) as labels which allows calculating uncertainties in a statistically optimal way. During training, a CDF is calculated for each original fluence correction label $\phi_c(v)$ and presented to the model and when estimating previously unseen data, the model predicts a CDF corresponding to the feature vector and an estimate of $\phi_c(v)$ can be reconstructed from the 50% percentile of said CDF estimation.

2.2 Confidence estimation

In machine learning applications, the main sources of uncertainty can be differentiated as aleatoric uncertainty U_a and epistemic uncertainty U_e.[12,14,21,22] U_a describes the inherent noise and is introduced by the imaging modality, whereas U_e represents the model uncertainty mainly introduced by invalid assumptions or the lack of training data. In this paper we represent these uncertainties as confidence metrics $C(v)$ on a voxel v bases, where lower values of $C(v)$ represent lower confidence and higher $C(v)$ represent higher confidence in the estimates.

Like any other medical imaging modality, PAT suffers from characteristic artifacts and noise pollution of recorded images. One way of encapsulating the noise inherent in PA images in an aleatoric confidence metric $C_a(v)$ is to use the inherent contrast-to-noise ratio (CNR) for example using a definition as suggested by Welvaert and Rossel[23]

$$\mathrm{CNR}(v) = \frac{S(v) - \mu_{noise}}{\sigma_{noise}} \tag{1}$$

with μ_{noise} and σ_{noise} being the mean and standard deviation of the background noise. We use this and calculate the standard score normalized confidence metric $C_a(v)$ as follows:

$$C_a(v) = \frac{\mathrm{CNR}(v) - mean(\mathrm{CNR})}{std(\mathrm{CNR})} \tag{2}$$

Using this definition, a low $C_a(v)$ indicates a low contrast-to-noise ratio, which would probably lead to a high absorption coefficient estimation error when performing fluence correction.

In contrast to $C_a(v)$, a metric of epistemic confidence $C_e(v)$ has to reflect the model uncertainty, for example caused, for example, by lack of knowledge in form of labelled training data during model creation. We use two confidence metrics to represent the epistemic uncertainty. The first is derived from the CDFs used as labels as described in section 2.1. Here, the $p_{0.8413}$ percentile and the $p_{0.1587}$ percentile of the CDF are calculated and used as the left and right error intervals to encapsulate the values within one standard deviation of the mean. Thus, a simple measure of uncertainty derived of the error intervals is $U_{e1}(v) = p_{0.8413}(\mathrm{CDF}(v)) - p_{0.1587}(\mathrm{CDF}(v))$ and a normalized confidence metric $C_{e1}(v)$ can be calculated with

$$C_{e1}(v) = -\frac{U_{e1}(v) - mean(U_{e1})}{std(U_{e1})} \tag{3}$$

Additionally, we use a second model to estimate the quantification performance of the proposed approach. In this case, to estimate a confidence metric $C_{e2}(v)$ for a previously unseen image, a random forest regressor is trained on feature vectors from the same training dataset $\mathrm{DS}_{\mathrm{train}}$ as the regressor used for estimating the optical property of interest. However, this time the feature vectors are labeled with the relative fluence estimation error in the training dataset $\mathrm{DS}_{\mathrm{train}}$:

$$E_{\mathrm{train}}(v) = \frac{|\hat{\phi}(v) - \phi(v)|}{\phi(v)} \tag{4}$$

where $\phi(v)$ is the ground truth fluence in v and $\hat{\phi}(v)$ is the fluence estimated by the model. Normalized estimations $\hat{E}_{\text{train}}(v)$ of this error can then be used as confidence metric $C_{e2}(v)$ with

$$C_{e2}(v) = -\frac{\hat{E}_{\text{train}}(v) - mean(E_{train})}{std(E_{train})} \tag{5}$$

where $E_{\text{train}} = \{e_{\text{r}}^{\phi}(v')|v' \in V_{\text{train}}\}$ is the set of all relative fluence estimation errors in DS_{train} with voxels V_{train}. The parameters of the regressor for confidence estimation are set to the same values as those of the first regressor.

In order to give one global confidence estimate for a single voxel estimation, the presented metrics need to be combined into one. As both C_{e1} and C_{e2} are estimates for the epistemic confidence of the machine learning algorithm, the average of both confidence estimates is calculated and interpreted as a metric of the overall epistemic confidence:

$$C_e(v) = \frac{C_{e1}(v) + C_{e2}(v)}{2} \tag{6}$$

To combine the epistemic and aleatoric confidence metric into one joint confidence metric C_j, the epistemic and aleatoric confidence measures are averaged as well. This is possible, as both $C_a(v)$ and $C_e(v)$ are in the same value range after the application of standard score normalization.

$$C_j(v) = \frac{C_a(v) + C_e(v)}{2} \tag{7}$$

2.3 Experiment

The purpose of our experiment is to validate whether incorporating the proposed confidence metric provides a benefit in terms of fluence estimation and absorption quantification accuracy. We use an *in silico* dataset for training of the machine learning algorithm. The dataset consists of multiple vessels in a homogeneous background. In each volume there are $1-7$ vessels that have a radius of $0.5-6$ mm and an absorption coefficient range of $1-12$ cm^{-1}. Light propagation is simulated using an adaptation of the widely used Monte Carlo framework *mcxyz* by Steve Jacques.[24] After simulation of the initial pressure distribution, we apply a Gaussian noise model with an additive component with a mean and std of 5 ± 5 a.u. corresponding to the average signal and a multiplicative component of 3%. This is done to resemble the noise levels commonly seen with our PA scanner.

For the concrete implementation of the epistemic confidence we followed the suggestions by Feindt[13] and use 100 sample points of the corresponding CDF as a label for the model. As the model we use the python scikit-learn[25] random forest implementation to estimate a CDF according to a given feature vector. During estimation, the fluence value can be reconstructed from the 50% percentile of the estimated CDF. Due to the nature of our data, we performed data augmentation by converting the label range into a logarithmic scale and sampled equally from the resulting distribution. At sampling time, we also applied random 20% white multiplicative Gaussian noise permutations of the feature vector for each sampled data item to prevent overfitting.

For hyperparameter adjustment, we monitor the training process on a validation dataset and report results on a separate test dataset. We evaluate the performance of the defined confidence metrics on all voxels as well as voxels in a certain region of interest (ROI), which is defined as all voxels within vessel structures with a CNR $>= 2$ as in previous work[20] where also more detailed information on the dataset simulation can be found.

3. RESULTS

We report quantitative results for both fluence estimation as well as absorption quantification and we define the relative fluence estimation error as e_{r}^{ϕ} and the relative absorption quantification error as $e_{\mathrm{r}}^{\mu_a}$. As the epistemic confidence metric C_e should be positively correlated with the relative fluence estimation error e_{r}^{ϕ}, because it is a measure of the uncertainty introduced by the machine learning model, we first evaluate the top n % confident samples according to C_e in section 3.1 and afterwards we evaluate the top n % confident absorption quantifications according to the joint confidence metric C_j in section 3.2. Figure 2 shows representative example images displaying examples of the epistemic as well as the joint confidence metric from the test dataset with the overall highest, lowest and median relative fluence estimation error in the CNR based region of interest (ROI).

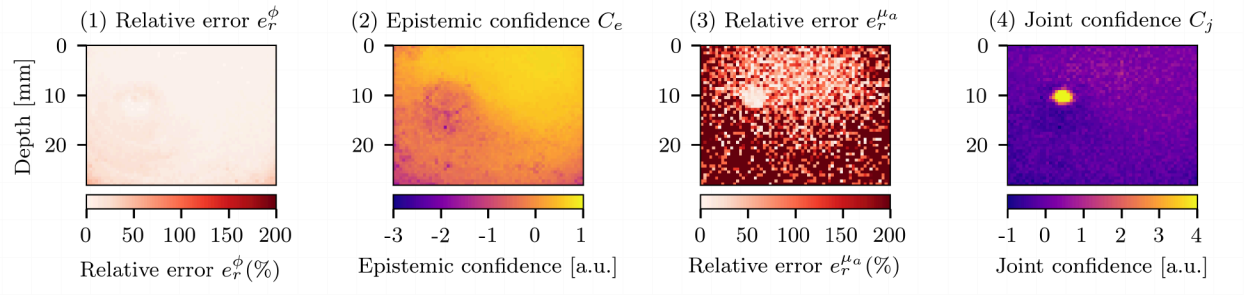

(a) Image with the lowest relative error

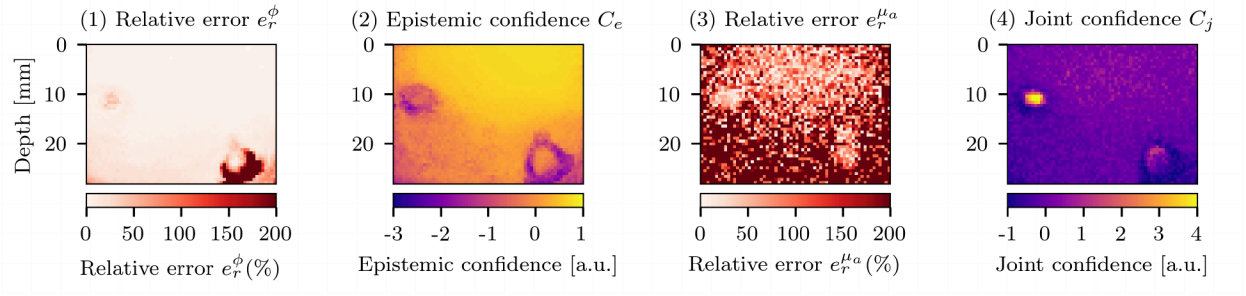

(b) Image with median relative error

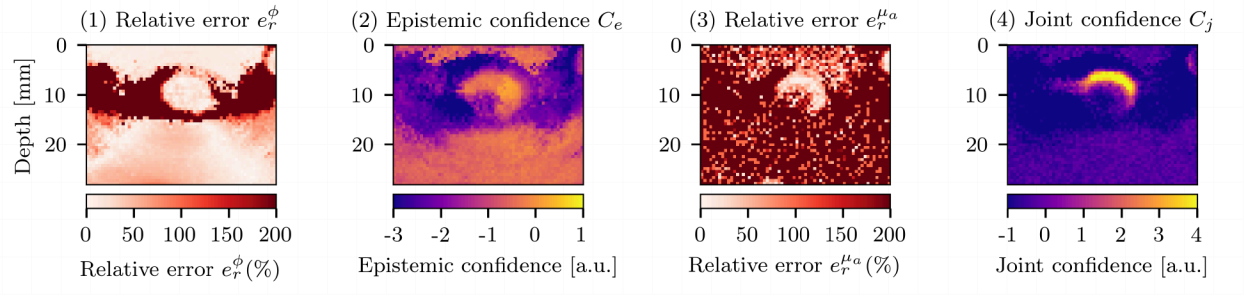

(c) Image with the highest relative error

Figure 2. Representative example images from the test dataset with the overall highest, lowest and median relative fluence estimation error in the CNR based region of interest (ROI). From left to right: (1) the relative fluence estimation error as well as (2) the corresponding epistemic confidence metric, (3) the relative absorption quantification error, and (4) the corresponding joint confidence metric. In (1) and (3) the darker shades of red correspond to higher relative estimation errors and in (2) and (4) high confidence corresponds to brighter yellow and orange colors whereas lower confidence values correspond to darker red and purple colors.

3.1 Epistemic confidence metric for fluence estimation

When considering all voxels, the results in this work correspond with the results presented in our previous work[20] for the high noise, multivessel dataset. In evaluation of the 2.5% most confident estimations, the median relative fluence estimation error e_r^{ϕ} over ROI dropped by up to 12 percentage points to 12% and by up to 5 percentage points to 0.7% when evaluating over all voxels (see figure 3).

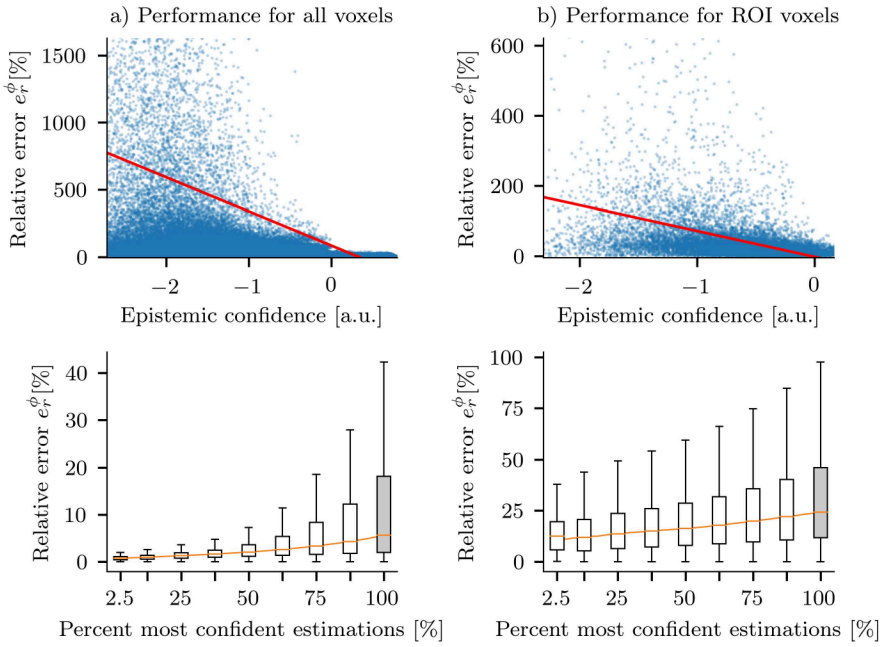

Figure 3. Evaluation of top n percent most confident estimations only. The top scatterplot shows the distribution of the relative estimation error in relation to the confidence measure. The boxplots demonstrate the distributions of the 2.5% to 100% most confident voxels. a) is evaluated over all voxels whereas b) shows the results when evaluating only over ROI voxels. In both cases there is an increasing improvement when evaluating over fewer more confident estimates. The red line represents the trendline of the data and the orange line plots the median errors.

3.2 Joint confidence metric for absorption reconstruction

The accuracy of absorption quantification is dependent on both the fluence estimation error as well as the noise of the PA image. Due to this dependency, the quantification error should be dependent on both the epistemic and the aleatoric confidence metrics.

We perform this evaluation by relating the relative absorption quantification error $e_r^{\mu_a}$ to the joint confidence metric C_j. When evaluating over the 2.5% most confident estimations, $e_r^{\mu_a}$ over ROI voxels dropped by 24 percentage points to 17% and by 107 percentage points to 41% when evaluating over all voxels (see figure 4).

3.3 Fourfold partitioning analysis of confidence metrics

In order to gain a better understanding of the properties of the presented confidence metrics we did a fourfold partitioning of their respective performances in the ROI (cf. fig. 5). When using the mean confidence and the median relative error as the partitioning values, the analysis revealed that for both metrics, nearly 70% of the tuples are either located in the high confidence low error or the low confidence high error quadrant. The remaining 30% of tuples are distributed in the other quadrants. The calculation of the mean absorption coefficients of each quadrant reveals that there is a positive correlation between the epistemic confidence and the absorption coefficient in fluence estimation as well as a negative correlation between the absorption coefficient and the absorption estimation error.

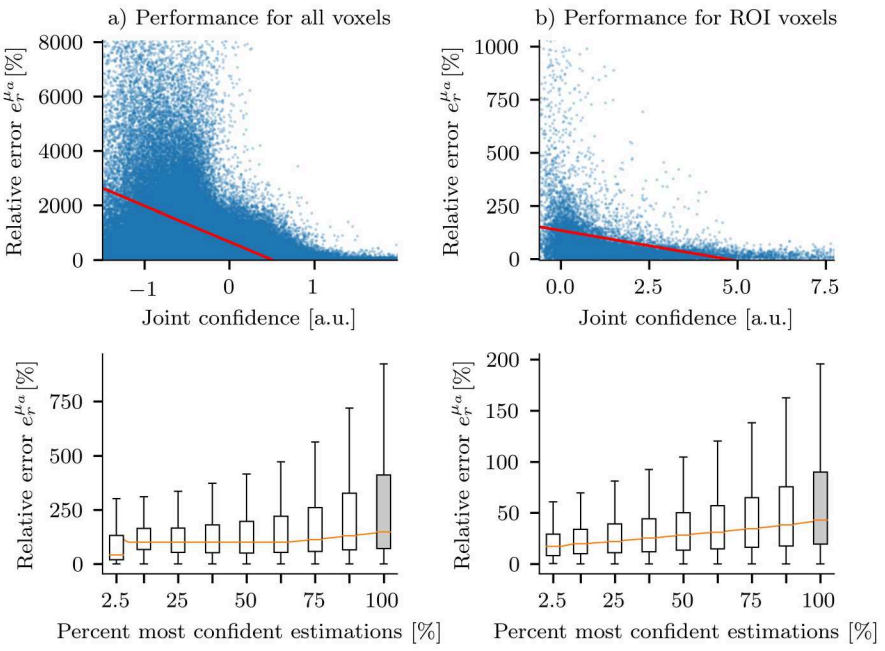

Figure 4. Evaluation of the n percent most confident quantifications over a) all and b) ROI voxels according to the joint confidence metric C_j. The distributions of the 2.5% to 100% most confident voxels are shown in boxplots. The red line represents the trendline of the data and the orange line plots the median errors.

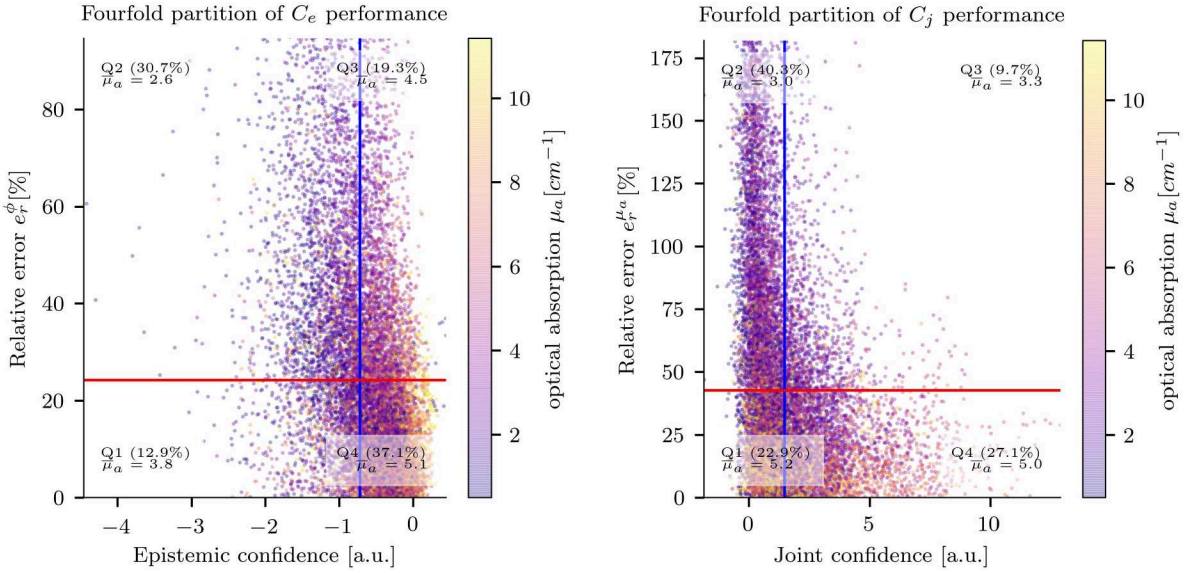

Figure 5. Fourfold partition of the (1) epistemic confidence metric and the relative fluence estimation error e_r^{ϕ} as well as the (2) joint confidence metric and the absorption estimation error $e_r^{\mu_a}$ in the ROI. The blue line represents is positioned at the mean confidence value and the red line is positioned at the median relative error. Nearly 70% of all tuples are located in Q2 and Q4, while 30% are located in Q1 and Q3. The color coding of the tuples corresponds to the corresponding optical absorption property.

4. DISCUSSION

The presented approach to confidence estimation provides a means to combine both epistemic and aleatoric confidences in a joint confidence metric for quantitative photoacoustic imaging. It would be a valuable tool for providing quantification results only for voxels with low estimated error. In this context, the tradeoff between the percentage of confident voxels and the increase in accuracy must be considered. It is worth noting that even a small percentage of very accurately quantified voxels can be utilized to obtain an improved measure of optical absorption or oxygenation in a region, as estimating optical and functional properties in larger regions is common in many imaging systems (cf. e.g.[26,27]). Doing so can yield an improvement over the practice of thresholding based on simply the signal intensity. In this contribution we suggest using the CNR as a metric for the aleatoric confidence. However, it is entirely possible to also use other signal-to-noise or contrast-to-noise metrics as defined by Welvaert and Rossel.[23] Completely different approaches as described by e.g. Kendall and Gal[12] are also viable. Figure 4 shows that the joint confidence metric might not be ideal when evaluating over all voxels and not over the pre-selected ROI. It is the intention of this project to provide thorough investigation into this aspect in future research. This is imperative, especially considering the rise in median error just before when evaluating on more than 2.5% but less than 10% of all voxels. This is most likely due to the fact that we calculate the CNR using the mean and std noise of the entire image. As such, this could be improved by using a separate noise model for each individual pixel in the imaging plane. Visualization of the joint confidence metric in figure 2 shows that the aleatoric confidence metric seems to outweigh the model-based confidence metric. This is understandable, as the proposed quantification strategy in fact amplifies additive noise components in regions with a low CNR. In this context it needs to be kept in mind that there are countless possible strategies of combining both the epistemic and aleatoric confidence metric and there may be aggregations favourable to the one presented in this work. The fourfold partitioning analysis shows the strengths and weaknesses of the proposed approach. The quadrants Q2 and Q4 are the quadrants representing high confidence and low error or low confidence and high error. While most confidence-error tuples are located in these quadrants, about 30% of all tuples are not. These are distributed into the two remaining quadrants: Q1 containing low confidence and low error and Q3 containing high confidence and high error. Cases where high errors are assigned a high confidence value can be very critical and thus need to be minimized. Using the joint confidence metric, these cases could be reduced from 19% to 10% with respect to using the epistemic confidence metric only. The proposed confidence metrics can potentially be provided in real-time, as they are directly derivable from either the PA image or the CDF estimates. An open question for future research is how to find a means of enabling a quantitative and data-independent interpretation of the proposed joint confidence metric. As in the currently proposed implementation the individual metrics are normalized over the entire test set before aggregation into the joint confidence C_j metric, the only practical approach is to consider a certain percentage of confident voxels, regardless of their actual value. However, it would be much more convenient to be able to have a fixed value range, wherein a certain value always corresponds to a high or low confidence estimation. This would enable calculation of matchable certainty estimates for any new quantification result. Furthermore, it has to be analyzed how the proposed epistemic confidence metric performs for hand-picked factitious tissue properties that were not included in the original training set. A thorough analysis of different quantification models in combination with the proposed confidence metrics would also be of interest.

The results of the performed experiment show that evaluation of a subset of very confident estimates can drastically improve accuracy. The validation was performed on Monte Carlo simulated *in silico* data, but if our findings hold true *in vitro* and *in vivo*, real-time provision of confidence metrics could prove to be an invaluable tool for clinical applications of qPAI.

ACKNOWLEDGMENTS

The authors would like to acknowledge support from the European Union through the ERC starting grant COMBIOSCOPY under the New Horizon Framework Programme grant agreement ERC-2015-StG-37960. The authors would also like to thank the ITCF of the DKFZ for the provision of their computing cluster.

REFERENCES

[1] Cox, B., Laufer, J. G., Arridge, S. R., and Beard, P. C., "Quantitative spectroscopic photoacoustic imaging: a review," *Journal of biomedical optics* **17**(6), 0612021–06120222 (2012).

[2] Xu, M. and Wang, L. V., "Photoacoustic imaging in biomedicine," *Review of scientific instruments* **77**(4), 041101 (2006).

[3] Ntziachristos, V., "Going deeper than microscopy: the optical imaging frontier in biology," *Nature Methods* **7**, 603–614 (Aug. 2010).

[4] Elbau, P., Mindrinos, L., and Scherzer, O., "Quantitative reconstructions in multi-modal photoacoustic and optical coherence tomography imaging," *Inverse Problems* (2017).

[5] Kaplan, B., Buchmann, J., Prohaska, S., and Laufer, J., "Monte-Carlo-based inversion scheme for 3d quantitative photoacoustic tomography," *Proceedings of the SPIE, Volume 10064, id. 100645J 13 pp.(2017).* **64** (2017).

[6] Tarvainen, T., Pulkkinen, A., Cox, B. T., and Arridge, S. R., "Utilising the radiative transfer equation in quantitative photoacoustic tomography," **10064**, 100643E–100643E–8 (2017).

[7] Brochu, F. M., Brunker, J., Joseph, J., Tomaszewski, M. R., Morscher, S., and Bohndiek, S. E., "Towards Quantitative Evaluation of Tissue Absorption Coefficients Using Light Fluence Correction in Optoacoustic Tomography," *IEEE Transactions on Medical Imaging* **36**, 322–331 (Jan. 2017).

[8] Haltmeier, M., Neumann, L., Nguyen, L. V., and Rabanser, S., "Analysis of the Linearized Problem of Quantitative Photoacoustic Tomography," *arXiv preprint arXiv:1702.04560* (2017).

[9] An, L., Saratoon, T., Fonseca, M., Ellwood, R., and Cox, B., "Statistical independence in nonlinear model-based inversion for quantitative photoacoustic tomography," *Biomedical Optics Express* **8**, 5297–5310 (Nov. 2017).

[10] Fonseca, M., Saratoon, T., Zeqiri, B., Beard, P., and Cox, B., "Sensitivity of quantitative photoacoustic tomography inversion schemes to experimental uncertainty," in [*SPIE BiOS*], 97084X–97084X, International Society for Optics and Photonics (2016).

[11] Pulkkinen, A., Cox, B. T., Arridge, S. R., Kaipio, J. P., and Tarvainen, T., "Estimation and uncertainty quantification of optical properties directly from the photoacoustic time series," **10064**, 100643N–100643N–7 (2017).

[12] Kendall, A. and Gal, Y., "What Uncertainties Do We Need in Bayesian Deep Learning for Computer Vision?," *arXiv:1703.04977 [cs]* (Mar. 2017).

[13] Feindt, M., "A Neural Bayesian Estimator for Conditional Probability Densities," *arXiv:physics/0402093* (Feb. 2004).

[14] Senge, R., Bösner, S., Dembczyski, K., Haasenritter, J., Hirsch, O., Donner-Banzhoff, N., and Hüllermeier, E., "Reliable classification: Learning classifiers that distinguish aleatoric and epistemic uncertainty," *Information Sciences* **255**, 16–29 (Jan. 2014).

[15] Gal, Y., Islam, R., and Ghahramani, Z., "Deep Bayesian Active Learning with Image Data," *arXiv:1703.02910 [cs, stat]* (Mar. 2017).

[16] Choi, S., Lee, K., Lim, S., and Oh, S., "Uncertainty-Aware Learning from Demonstration using Mixture Density Networks with Sampling-Free Variance Modeling," *arXiv:1709.02249 [cs]* (Sept. 2017).

[17] Maier-Hein, L., Ross, T., Gröhl, J., Glocker, B., Bodenstedt, S., Stock, C., Heim, E., Götz, M., Wirkert, S., Kenngott, H., and others, "Crowd-algorithm collaboration for large-scale endoscopic image annotation with confidence," in [*International Conference on Medical Image Computing and Computer-Assisted Intervention*], 616–623, Springer (2016).

[18] Moccia, S., Wirkert, S. J., Kenngott, H., Vemuri, A. S., Apitz, M., Mayer, B., De Momi, E., Mattos, L. S., and Maier-Hein, L., "Uncertainty-Aware Organ Classification for Surgical Data Science Applications in Laparoscopy," *arXiv:1706.07002 [cs]* (June 2017). arXiv: 1706.07002.

[19] Tarvainen, T., Pulkkinen, A., Cox, B. T., Kaipio, J. P., and Arridge, S. R., "Image reconstruction with noise and error modelling in quantitative photoacoustic tomography," in [*SPIE BiOS*], 97083Q–97083Q, International Society for Optics and Photonics (2016).

[20] Kirchner, T., Gröhl, J., and Maier-Hein, L., "Local context encoding enables machine learning-based quantitative photoacoustics," *arXiv:1706.03595 [physics]* (June 2017).

[21] Urbina, A., Mahadevan, S., and Paez, T. L., "Quantification of margins and uncertainties of complex systems in the presence of aleatoric and epistemic uncertainty," *Reliability Engineering & System Safety* **96**, 1114–1125 (Sept. 2011).

[22] Chowdhary, K. and Dupuis, P., "Distinguishing and integrating aleatoric and epistemic variation in uncertainty quantification," *ESAIM: Mathematical Modelling and Numerical Analysis* **47**, 635–662 (May 2013).

[23] Welvaert, M. and Rosseel, Y., "On the Definition of Signal-To-Noise Ratio and Contrast-To-Noise Ratio for fMRI Data," *PLOS ONE* **8**, e77089 (June 2013).

[24] Jacques, S. L., "Coupling 3d Monte Carlo light transport in optically heterogeneous tissues to photoacoustic signal generation," *Photoacoustics* **2**(4), 137–142 (2014).

[25] Pedregosa, F., Varoquaux, G., Gramfort, A., Michel, V., Thirion, B., Grisel, O., Blondel, M., Prettenhofer, P., Weiss, R., Dubourg, V., and others, "Scikit-learn: Machine learning in Python," *Journal of Machine Learning Research* **12**(Oct), 2825–2830 (2011).

[26] Tzoumas, S., Nunes, A., Olefir, I., Stangl, S., Symvoulidis, P., Glasl, S., Bayer, C., Multhoff, G., and Ntziachristos, V., "Eigenspectra optoacoustic tomography achieves quantitative blood oxygenation imaging deep in tissues," *Nature Communications* **7**, 12121 (June 2016).

[27] Valluru, K. S., Wilson, K. E., and Willmann, J. K., "Photoacoustic Imaging in Oncology: Translational Preclinical and Early Clinical Experience," *Radiology* **280**, 332–349 (July 2016).